Pharm Res (2011) 28:2119–2129
DOI 10.1007/s11095-011-0437-2

RESEARCH PAPER

Modelling Dermal Drug Distribution After Topical Application in Human

Yuri G. Anissimov • Michael Stephen Roberts

Received: 23 December 2010 / Accepted: 21 March 2011 / Published online: 27 April 2011

ABSTRACT

Purpose To model and interpret drug distribution in the dermis and underlying tissues after topical application which is relevant to the treatment of local conditions.

Methods We created a new physiological pharmacokinetic model to describe the effect of blood flow, blood protein binding and dermal binding on the rate and depth of penetration of topical drugs into the underlying skin. We used this model to interpret literature *in vivo* human biopsy data on dermal drug concentration at various depths in the dermis after topical application of six substances. This interpretation was facilitated by our *in vitro* human dermal penetration studies in which dermal diffusion coefficient and binding were estimated.

Results The model shows that dermal diffusion alone cannot explain the *in vivo* data, and blood and/or lymphatic transport to deep tissues must be present for almost all of the drugs tested.

Conclusion Topical drug delivery systems for deeper tissue delivery should recognise that blood/lymphatic transport may dominate over dermal diffusion for certain compounds.

KEY WORDS dermal drug distribution · modelling · percutaneous penetration · topical drug delivery

Y. G. Anissimov (✉)
School of Biomolecular and Physical Sciences, Griffith University
Gold Coast, Queensland 4222, Australia
e-mail: Y.Anissimov@Griffith.edu.au

M. S. Roberts
School of Medicine
University of Queensland, Princess Alexandra Hospital
Brisbane, Queensland 4102, Australia

M. S. Roberts
School of Pharmacy and Medical Sciences
University of South Australia
Adelaide, South Australia 5001, Australia

INTRODUCTION

Drugs and other solutes are frequently applied to the skin for a range of purposes, including the treatment of local dermatological disorders, systemic delivery (e.g. nicotine, nitroglycerin, fentanyl patches), supportive treatment of local muscle injuries, cosmetic, UV protection and insect repellents. This interest in topical applications of pharmaceutical and cosmetic products has generated significant research effort into measurement, modelling and prediction of the rate of solute penetration through the skin. The research effort into understanding the distribution of topically applied solutes in underlying tissues has been relatively modest, confounded by the inability to recreate *in-vivo* conditions using *in-vitro* experiments (1) and the invasiveness associated with the collection of such data using biopsy. Most prominent in this regard is the work of Schaefer and colleagues, who obtained human tissue concentration-depth profiles of various drugs *in-vivo* after topical application (1–5).

As studies on skin solute concentration–tissue depths profiles after topical application in human are, in general, limited due to the invasiveness associated with the collection of such data, mathematical modelling and prediction of concentration-depths profiles for different drugs are of importance in dermatology. Singh and Roberts (6,7) have used compartmental pharmacokinetic model assuming first-order diffusional mass transfer between the dermis and underlying tissue compartments with its concurrent elimination due to blood flow to model salicylic acid distribution in rat after topical application. Later, Gupta *et al.* (8) successfully modelled spatial distribution of 2′,3′-dideoxyinosine in the dermis of a rat using a distributed elimination model. Cross and Roberts (9) used a tissue diffusion-dermal blood flow clearance model similar to the model of Gupta *et*

al. (8) but taking into account declining concentration in the donor phase to describe drug distribution kinetics in wound tissue after topical application. Recently, the data of Singh and Roberts (7) was reanalysed with a similar distributed diffusion-clearance model by Kretsos *et al.* (10) and found to be consistent with this model. Kretsos and Kasting (11) also developed a new model to describe the dermal capillary clearance process based on assumed periodic microscopic distribution of dermal capillaries in three-dimensional space. This model yields localised concentration in the dermis, but so far only applies to the steady-state case.

In this work, we developed a new model that takes into account transport to deeper tissues by blood and/or lymphatics. The model also includes the potential contribution to transport processes by dermal diffusion and vascular wall permeability. We use a combination of human biopsy data generated by Schaefer and colleagues (1–5) and our own human *in-vitro* dermis penetration experiments to obtain two critically important parameters of the distributed model: dermis diffusion/dispersion coefficient and dermal blood clearance rate for six solutes: Desoximetasone (Des), Econazole (Ec), Hydrocortisone (Hyd), 8-Methoxypsoralen (Met), Retinoic acid (RA), Triamcinolone acetonide (TA) (molecular weight, solubility and other physicochemical properties of this solutes are presented in Table I).

THEORY

In Vivo Dermal Distribution Model

The distributed elimination model (8,9,12) is often used to describe dermis concentration-depth profiles and is similar to the model previously introduced for peritoneum by Dedrick *et al.* (13). These previous studies have assumed all solute transport to deeper layers occurs by molecular diffusion. The distributed elimination model defines concentration in the dermis by the diffusion equation with elimination:

$$\frac{\partial C_d}{\partial t} = D\frac{\partial^2 C_d}{\partial x^2} - k_e C_d \tag{1}$$

where $C_d(x,t)$ is the concentration of the solute in the layer of the dermis at depth x at time t, D is the effective molecular diffusion coefficient in the dermis and k_e is an assumed elimination rate from the dermis. An alternative to the molecular diffusion of the solute is that D is a dispersion term used widely in chemical engineering (14) and in organ pharmacokinetics (15) and defines transport by both blood and diffusion in the dermis. Partitioning of solute into blood capillaries of the dermis and its subsequent convective transport and partitioning back into the tissue could also significantly contribute to the spatial transport of the solute. Blood in the tissue capillaries can flow in all possible directions; it can be argued that this repartitioning and convective transport of the solute will be similar to a random walk process. The lymphatic flow could also be a contributing factor to the solute tissue transport. In order to recognise these facts, D in Eq. 1 needs to be replaced by D_t:

$$D_t = D_v + D \tag{2}$$

where D_v is the contribution to the transport from blood and/or lymphatics. If the repartitioning and convective transport or lymphatic transport do contribute significantly to the transport of solute, D_v will be much greater than molecular diffusion coefficient (D). If the transport is dominated by molecular diffusion, then $D_t \approx D$. For the solute that is bound in the dermis, and only unbound solute is diffusing, the effective diffusion coefficient is defined as (16)

$$D = D_u f u_d \tag{3}$$

where D_u is the diffusion rate of unbound solute.

In Eq. 1, it is implicitly assumed that the elimination rate (k_e) is due to blood flow clearance, but hitherto no

Table I Physicochemical Properties of Solutes (mean ± SD, $n=4$)

Solute	MW[a]	log P[b]	S_r[c] ($\mu g.ml^{-1}$)	S_p[d] ($\mu g.ml^{-1}$)	S_b[e] ($\mu g.ml^{-1}$)	S_d[f] ($\mu g.ml^{-1}$)	S_w[g] ($\mu g.ml^{-1}$)	pKa[h]	$S_{w\ pH=7.4}$[i] ($\mu g.ml^{-1}$)
Desoximetasone	376.5	2.35	437 ± 43	474 ± 16	362 ± 18	787 ± 165	42.1	NA	42.1
Econazole	381.7	5.81[k]	332 ± 20	2,587 ± 82	1,968 ± 138	432 ± 126	5.0[j]	6.69[k]	6.0
Hydrocortisone	362.5	1.61	351 ± 22	446 ± 24	444 ± 24	625 ± 67	320.0	NA	320.0
8-Methoxypsoralen	216.2	2.14	213 ± 9	234 ± 7	199 ± 24	277 ± 54	47.6	NA	47.6
Retinoic acid	300.4	6.30	104 ± 4	146 ± 3	109 ± 4	41 ± 12	0.126	4.8	1.3
Triamcinolone acetonide	434.5	2.53	43.2 ± 0.6	56 ± 3	53 ± 1	73 ± 5	21.0	NA	21.0

[a] *MW* molecular weight; [b] *log P* log octanol-water partition coefficient; [c] S_r solubility in receptor/donor solution; [d] S_p solubility in blood plasma; [e] S_b solubility in the blood; [f] S_d solubility in the dermis; [g] S_w solubility in water; [h] *pKa* log acid dissociation constant; [i] $S_w\ pH_{7.4}$ solubility in water when pH is maintained at pH = 7.4; [j] From (2); [k] Calculated value from SciFinder Scholar

connections to physiological parameters made it difficult to analyse physiological meaning of this parameter. In order to relate this elimination rate to such physiological parameters as blood flow in the dermis and permeability surface area of blood capillaries in the dermis, we consider a simple two-compartmental approach to diffusion/dispersion in the dermis and elimination by blood flow in the small volume of the dermis (V_d) at depth x (see Fig. 1). Equations which describe the diffusion/dispersion in the dermis compartment and partitioning into the adjacent blood compartment with subsequent elimination are

$$V_d \frac{\partial C_d}{\partial t} = V_d D_t \frac{\partial^2 C_d}{\partial x^2} - PS(C_d fu_d - C_b fu_b) \tag{4}$$

$$V_b \frac{dC_b}{dt} = -Q_b C_b + PS(C_d fu_d - C_b fu_b) \tag{5}$$

where V_b is the blood volume adjacent to the dermis, Q_b is the blood flow rate in the volume V_d, and PS is the permeability surface area product (PS, sometimes abbreviated as PA), which is standard term in pharmacokinetics that consists of the permeability coefficient (P) often used to describe the transport of various solutes across the capillary wall multiplied by the surface area of the wall (S) in the volume V_d. Further, C_b is the concentration of solute in blood compartment; fu_d and fu_b are fractions of solute unbound in the dermis and blood. In Eq. 5 it was assumed that fresh arterial blood reaching the skin does so without any solute present ($C_{b0}=0$). The boundary conditions for $C_d(x, t)$ are

$$-D_t \frac{\partial C_d}{\partial x}|_{x=0} = J_0 \tag{6}$$

$$\lim_{x\to\infty} C_d(x,t) = 0 \tag{7}$$

and represent the flux (J_0) through the epidermal/dermal juncture (Eq. 6) and diminishing concentration in the deeper layers (Eq. 7).

It is important to emphasise that Eqs. 4 and 5 do not take into account the complex physiology of blood circulation in the skin (see Fig. 1a). The model that has a more detailed consideration of the capillaries in dermal clearance was developed by Kretsos and Kasting (11), but only applies to the steady-state case. The presented model can be viewed as a simplification of the approach of Kretsos and Kasting (11), which allows to model transient kinetics.

Partial differential Eqs. 4 and 5 with boundary conditions 6 and 7 could be solved in Laplace domain to yield

$$\widehat{C}_d(x,s) = \frac{J_0}{s\sqrt{(s+g(s))D_t}} \exp\left(-x\sqrt{(s+g(s))/D_t}\right) \tag{8}$$

where $\widehat{C}_d(x,s)$ is the Laplace transform of $C_d(x, t)$ and s is the Laplace variable. Further, the function $g(s)$ in Eq. 8 is defined as

$$g(s) = \frac{fu_d q_b ps + psfu_d v_b s}{q_b + fu_b ps + v_b s}$$

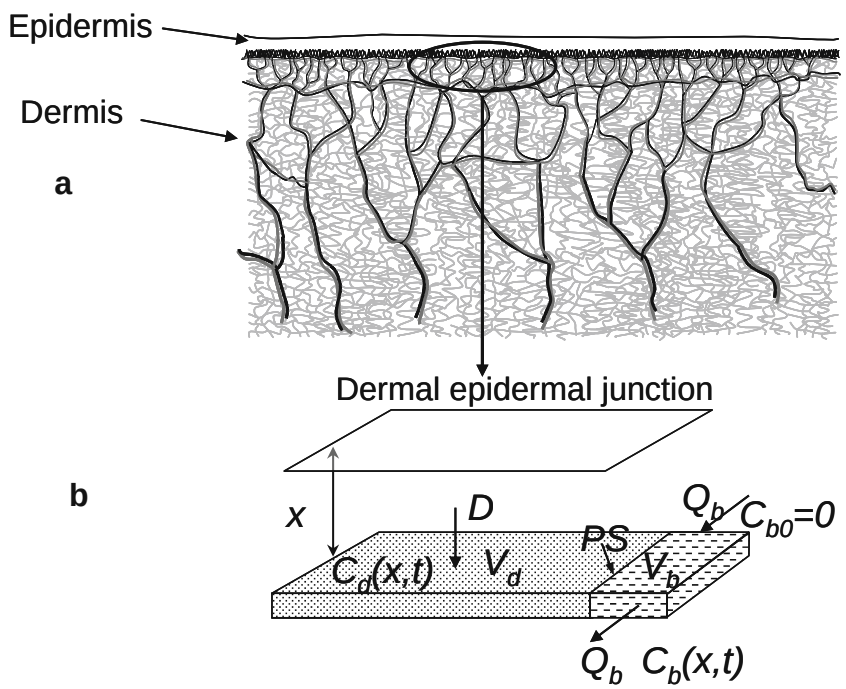

Fig. 1 Skin (**a**) and its schematic representation in the model (**b**).

where q_b, ps and v_b are the blood flow rate, the permeability surface area product for blood capillaries and blood capillaries volume per unit volume of dermis, respectively. In Eq. 8 the flux through epidermis (J_0) is assumed constant, but replacing J_0 with $J_0(t)$ in Eq. 6 and then J_0 with $\widehat{J}_0(s)$ in Eq. 8 allows the analysis for the case of the transient flux through epidermis.

For the steady-state case, the time derivatives in Eqs. 4 and 5 are zero, and C_b can be expressed in terms of C_d using Eq. 5; these can be substituted into Eq. 4 to yield

$$D_t \frac{\partial^2 C_d}{\partial x^2} - \frac{fu_d Q_b PS}{(Q_b + fu_b PS) V_d} C_d = 0 \tag{9}$$

Hence, at steady state, the form of the derived two-compartmental dermal distribution model is identical with the distributed elimination model (Eq. 1), except that the elimination rate can now be defined in terms of physiological parameters as follows:

$$k_e = \frac{fu_d Q_b PS}{(Q_b + fu_b PS) V_d} = \frac{fu_d q_b ps}{q_b + fu_b ps} \tag{10}$$

Kretsos *et al.* (12) arrived at a similar expression for k_e but did not recognise the effect that solute binding may have on the elimination rate.

It follows from Eq. 10 that when penetration of the solute into the blood capillary is the rate-limiting process, that is, $fu_b\ ps << q_b$, k_e will be determined by ps so that Eq. 10 simplifies to k_e being dependent on permeability surface area for blood capillaries ps:

$$k_e = fu_d ps \tag{11}$$

On the other hand, when blood flow q_b is rate limiting, ($fu_b\ ps >> q_b$), now Eq. 10 simplifies to k_e being dependent on tissue blood flow qb:

$$k_e = q_b fu_d / fu_b \tag{12}$$

Solving Eq. 9 with boundary conditions 6 and 7 yields the concentration of solute in the dermis for the steady state:

$$C_{ss}(x) = C_0 \exp(-k_d x) = \frac{J_0}{\sqrt{k_e D_t}} \exp\left(-x\sqrt{k_e / D_t}\right) \tag{13}$$

We note that Eq. 13 can also be obtained by taking a limit $C_{ss}(x) = \lim_{s \to 0} s\widehat{C}_d(x,s)$ where $\widehat{C}_d(x,s)$ is defined in Eq. 8. Using Eq. 10 the distribution parameter k_d can be defined in terms of physiological parameters of the model:

$$k_d = \sqrt{\frac{fu_d q_b ps}{D_t(q_b + fu_b ps)}} \tag{14}$$

MATERIALS AND METHODS

Materials

All chemicals (Des, Ec, Hyd, Met, RA, TA) were purchased from Sigma-Aldrich Chemie Gmbh (Steinheim, Germany).

Dermis Preparation Technique

Female abdominal skin was obtained following abdomnoplasty from two donors. Extraneous fat and subcutaneous tissue from the underside of the skin was removed by blunt dissection. Dermal membranes were prepared by removing epidermis using heat separation (immersion in water at 60° C for 1 min) from full-thickness skin.

In Vitro Penetration Studies

All studies were carried out in horizontal static Franz-type diffusion cells (receptor volume approximately 3.5 ml, surface area approximately 1.3 cm^2). Receptor compartments were filled with phosphate-buffered saline, pH 7.4, containing 4% bovine serum albumin (further referred to as receptor solution), maintained at 36°C in a water bath and continuously stirred with magnetic fleas. In this work, 4% bovine serum albumin was used to mimic typical albumin concentrations present in the blood, with identical concentrations being used on both sides of the dermis to avoid creating an albumin concentration gradient that could potentially lead to an osmotic flow of water through the dermis. Dermal membranes were equilibrated overnight at room temperature with receptor solution on both sides of the membrane before the start of experiments. Saturated solutions of chemicals in the receptor solution were used as donor solutions and were produced by stirring in orbital shaker excess amount of the chemical for at least 10 h. One ml of donor solution was applied at the start of the penetration experiment, and aliquots of 200 µl were taken from the receptor and replaced with fresh solution. Samples were then analysed by HPLC. These data were analysed by fitting the steady-state penetration equation to the steady-state section of the cumulative amount penetrated ($Q(t)$) *vs.* time experimental curve (17):

$$Q(t) = k_p C_0 A\left(t - t_{lag}\right) \tag{15}$$

where C_0 is the concentration of solute in the donor solution, A is the area of the dermis, k_p is the dermal permeability coefficient and t_{lag} is the lag time. The linear regression of the steady-state portion of the curve yielded two parameters, k_p and t_{lag}. These parameters are, in turn, defined by the partition coefficient between donor solution

and the dermis (K_m), the thickness of the dermis (h) and effective diffusion coefficient in the dermis (D) as (17):

$$k_p = \frac{K_m D}{h} \tag{16}$$

$$t_{lag} = \frac{h^2}{6D} \tag{17}$$

At the end of the penetration experiment, diffusion cells were dismantled, and the thickness of a dermal membrane (h) was determined by placing them between glass slides and measuring with callipers. Sections of the membrane exposed to the donor and receptor solutions was cut, weighed and put into 10 ml of fresh receptor solution. This solution was sampled after at least 16 h, its concentration measured with HPLC and amount of drug in the dermis determined. The partition coefficient between donor solution and the dermis (K_m) was determined from the amount of solute in the dermis (Am_{derm}) of mass m_{derm} after the penetration experiment assuming linear concentration gradient in the dermis (17):

$$K_m = \frac{2Am_{derm}\rho_{derm}}{C_0 m_{derm}} \tag{18}$$

where ρ_{derm} is the density of the dermis assumed to be 1 g/ml. Using Eqs. 16–18 diffusion coefficient was determined from both k_p and t_{lag}. We note that factor 2 in Eq.18 arises from the fact that concentration in the dermis reaches steady-state linear profile with concentration in contact with the donor being $K_m C_0$ and zero concentration at the contact with the receptor (sink condition).

Solubility Measurements

For receptor solution solubility (S_r) measurements, saturated donor solutions produced by stirring in orbital shaker excess amount of the chemical for at least 10 h were filtered (Millipore Millex Syringe Driven Filter, 0.22 μm), diluted 5 times with receptor solution, and measured with HPLC. Solubilities in human plasma (S_p) were measured similarly. To estimate solubility in human blood (S_b), partitioning between plasma and red blood cells (RBC) was measured: 1 ml of plasma with known drug concentration was mixed with 1 ml of RBC and incubated for at least 12 h, and then plasma concentration was measured. The total amount and concentration in RBC was then calculated and solubility in blood approximated assuming hematocrit of 0.5. The fraction unbound in the dermis (fu_d) and blood (fu_b) were estimated as the ratio of solubility in the water at pH=7.4 ($S_{w\ pH=7.4}$) to solubility in the dermis ($S_d=K_m S_r$) and solubility in the blood (S_b), respectively.

Analysis of Published *In Vivo* Study Data

Data were extracted from the published literature using Data Thief III (http://www.datathief.org/). In accordance with Eq. 13, data were expressed as a log-linear relationship of log of concentration *vs.* distance profiles for all solutes with the distribution parameter k_d determined as the negative value of the slope of the resulting linear relationship for steady-state data. Nonlinear regressions of data were performed using the program SCIENTIST (MicroMath Scientific software, Salt Lake City) with weighting of $1/y_{\mathrm{observed}}$.

HPLC Analysis

BSA in 200 μl receptor samples was precipitated using 300 μl of ACN with 50 μg/ml of internal standard (TA for Des, Met and Hyd; Des for Ec and TA; Benzyl Salicylate for RA). Samples were then centrifuged (Clements Orbital 100, Clements Medical Equipment Pty Ltd., Rydalmere, NSW, Australia) for 6 min at high speed and supernatant analysed by HPLC system (Shimadzu, Kyoto, Japan). The flow rate of 1 ml per minute was always used through a reverse phase C18 column (Waters® Symmetry C18, 5 μm, 150×3.9 mm) including a guard column (Phenomenex® C18, 4×3 mm). and 20 μl of sample was injected. Mobile phase was 40% ACN, 60% Phosphate buffer (20 mM KH_2PO_4 at pH=3 adjusted with H_3PO_4) for Ec, 35% ACN, 65% water for Hyd, 80% ACN, 20% Acetate buffer (5 mM $NaC_2H_3O_2$ at pH=2.7 adjusted with acetic acid) for RA and 40% ACN, 60%, water for other solutes. Retention times were 4.5, 6.6, 2.7, 4.1, 7.5 and 3.5 min for Des, Ec, Hyd, Met, RA and TA, respectively. Detection wavelengths were for Ec 230 nm, Hyd 254 nm, RA 354 nm and 245 nm for other solutes.

RESULTS

In Fig. 2, human literature data for concentration-depth profiles of six solutes are presented together with the results of the regression with the steady-state model (Eq. 13 with fitting parameters C_0 and k_d, solid line). Values for k_d from the regressions using the steady-state model are presented in Table II. The regression with the steady-state model yields satisfactory fits for most solutes, although the quality of the regression varies: there is lower regression quality for Desoximetasone (coefficient of determination: cd=0.54)

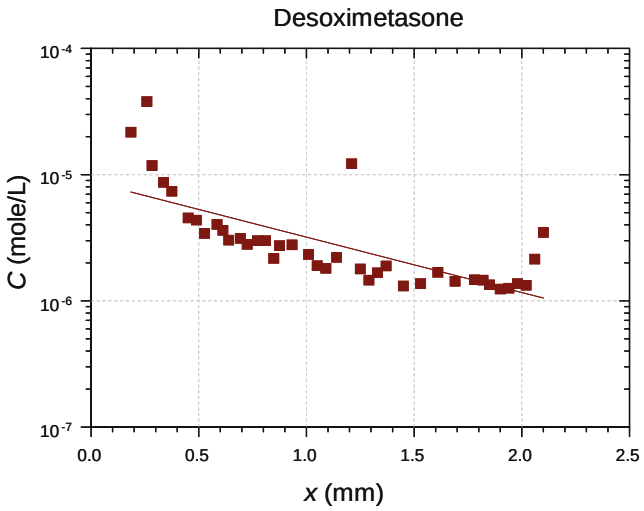
Desoximetasone
C (mole/L)
x (mm)

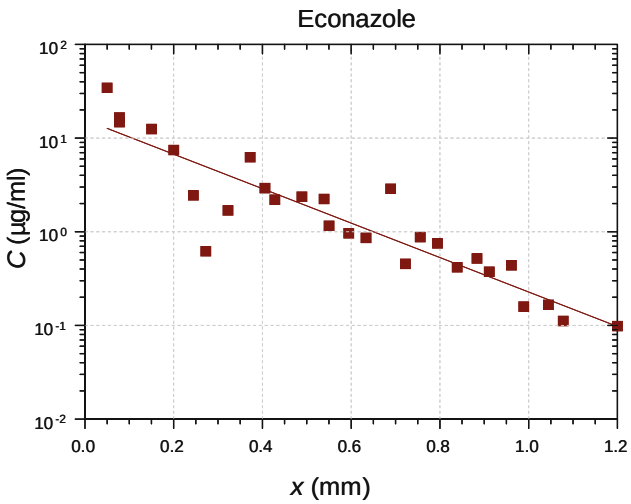
Econazole
C (µg/ml)
x (mm)

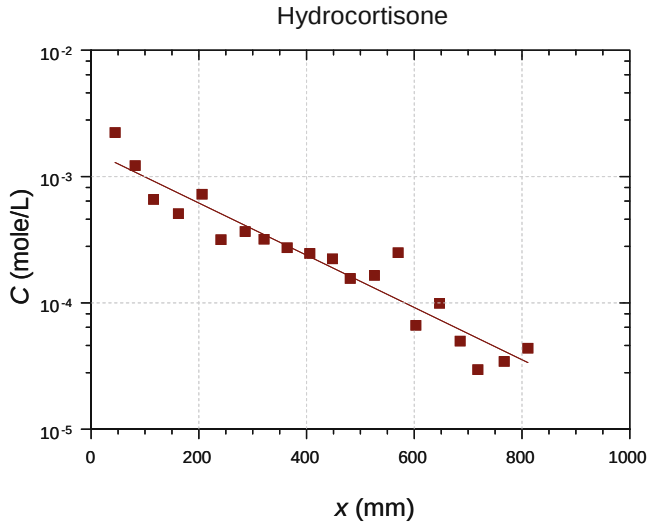
Hydrocortisone
C (mole/L)
x (mm)

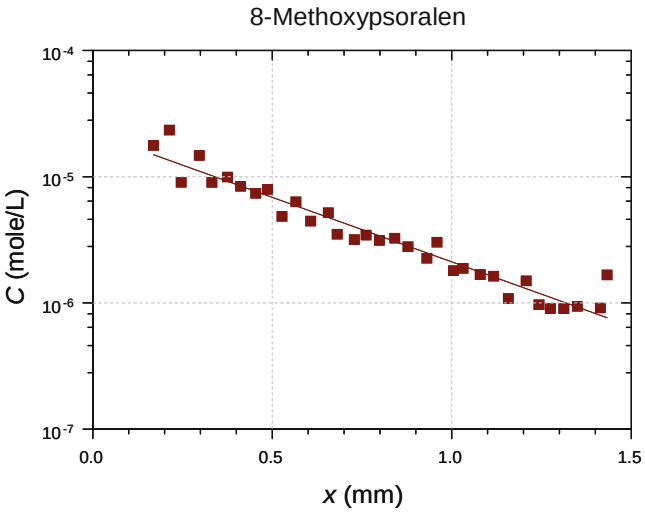
8-Methoxypsoralen
C (mole/L)
x (mm)

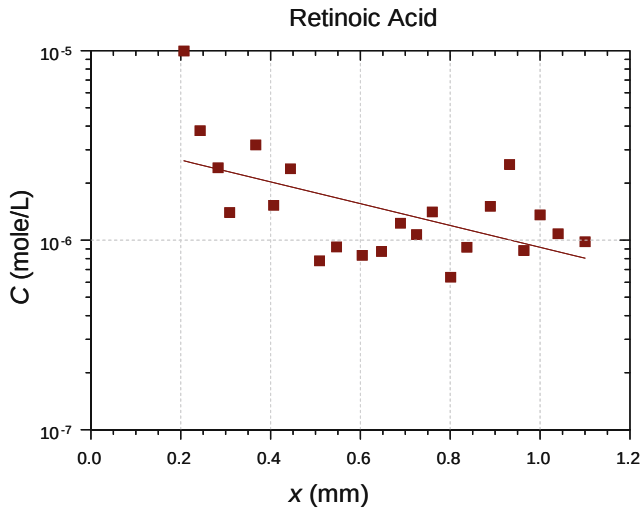
Retinoic Acid
C (mole/L)
x (mm)

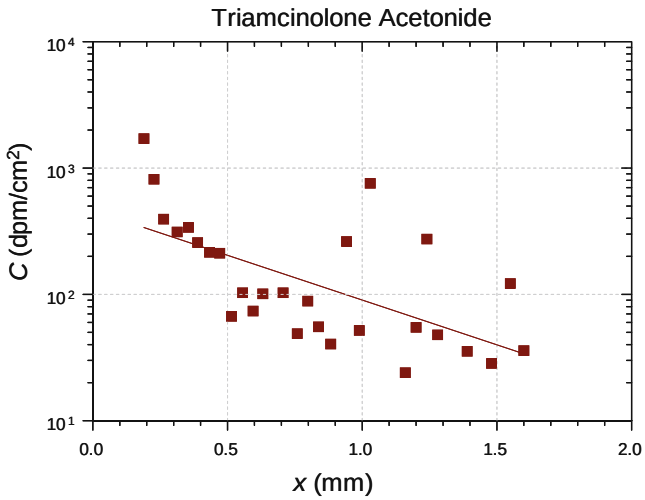
Triamcinolone Acetonide
C (dpm/cm²)
x (mm)

Fig. 2 Experimental data for dermal distribution of Desoximetasone (from (5), Fig. 5 after 1,000 min), Econazole (from (1), Fig. 2 application thigh after 90 min), Hydrocortisone (from (3), Fig. 1 after 1,000 min), 8-Methoxypsoralen (from (5), Fig. 6 after 100 min), Retinoic acid (from (2) Fig. 1 after 100 min), Triamcinolone acetonide (from (6) Fig. 1 after 100 min) and regression curves with the steady state model (Eq. 13). Coefficients of determination (cd) for each of the solute's regression and number of data points are as follows: Desoximetasone cd = 0.54, n = 40; Econazole cd = 0.84, n = 28; Hydrocortisone cd = 0.91, n = 20; 8-Methoxypsoralen cd = 0.94, n = 33; Retinoic acid cd = 0.33, n = 22; Triamcinolone acetonide cd = 0.39, n = 28.

Retinoic acid (cd = 0.33), and Triamcinolone acetonide (cd = 0.39) (poor regression quality is apparently due to larger variability of experimental data for these solutes) and is better for Ec, Hyd and Met, with coefficients of determination 0.84, 0.91, 0.94, respectively. It follows from the analysis of the new model (see Eq. 14) that k_d depends on different physiological parameters, such as D_b, ps, fu_b, fu_d and q_b, and for further investigation some of these parameters should be determined independently. This underpinned the necessity of investigating physicochemical properties of solutes together with human dermis *in vitro* experiments. In Table I physicochemical properties of solutes obtained from PhysProp database (Syracuse Research Corporation) and in our experiments are presented. It can be seen that the solutes cover a reasonably large range in terms of solute molecular weight (MW), logarithm of the solute's octanol/water partition coefficient (LogP) and solute solubility in water (S_w). We have measured solubility in the receptor/donor solution (S_r) in blood plasma (S_p) and in blood (S_b). Two solutes are partially ionised at the experimental conditions (pH = 7.4): Ec is a base, and RA is an acid, and therefore their effective solubility in the buffer at pH = 7.4 will be higher than that in water, especially for the acid RA.

It can be seen from Table I that the solubility in plasma for all solutes with the exception of Ec is higher but close to that in the receptor phase, which is consistent with receptor phase bovine serum albumin concentration being similar to that of blood. The much higher solubility in plasma and blood for Ec is probably due to its strong binding to some proteins other than albumin (which is present in the receptor phase).

Dermal partition, permeability and diffusion coefficients are derived from our *in vitro* dermal penetration studies and presented in Table II. It should be noted that K_m is the partitioning coefficient between dermis and the donor solution that contains 4% bovine serum albumin and that this partitioning coefficient can differ from $K_{dermis/water}$, especially for strongly protein-bound solutes. Diffusion coefficients were derived from both lag time and permeability coefficient and were found to be similar, with the exception of Met, for which there is about a factor of two difference between the two values. The fraction unbound in the dermis and blood was estimated as the ratio of solubility in the water at pH = 7.4 (Table I) to solubility in the dermis ($S_d = K_m S_r$) and solubility in the blood (S_b), respectively. Two of the solutes in Table II (Hyd and Met) were previously analysed by Kretsos *et al.* (12), using the same human data ((3) for Hyd and (5) for Met). They reported similar values for k_d (referred to in (12) as decay parameter E) to what we estimated in our analysis (*i.e.* k_d values of 43 cm^{-1} *vs.* 48 cm^{-1} for Hyd and 21 cm^{-1} *vs.* 24 cm^{-1} for Met).

Figure 3 shows dermal diffusion coefficients (D) plotted *versus* fractions of solute unbound in the dermis (fu_d). It can be seen that, with the exception of Des, all the solutes roughly fall onto the straight line in agreement with Eq. 3, with unbound diffusion coefficients being about the same for all solutes ($D_u \approx 10^{-6}$ $cm^2 s^{-1}$). This is expected, as D_u can be approximated by the solute diffusion in water, which is expected to be proportional to $MW^{-1/2}$ (18) (in (18) it is stated that diffusion coefficient is proportional to $MV^{-0.6}$, where MV is molecular volume; for simplicity we used an approximation $MW^{-1/2}$ here). Further, as the square root of molecular weight of solutes does not change significantly, D_u is expected to be roughly the same for all solutes. The deviation of diffusion coefficient for Des from the trend could be explained by its binding to some component of the skin capable of diffusing. This binding would decrease Des's fractions unbound in the dermis (fu_d = 0.054, see Table II),

Table II Solute Model Parameters for Transport in the Dermis (mean ± SD, n = 4)

Solute	k_d[a] (cm^{-1})	K_m[b]	k_p[c] $\times 10^3$ ($cm.h^{-1}$)	$D^d \times 10^7$ from t_{lag} ($cm^2.s^{-1}$)	$D^d \times 10^7$ from k_p ($cm^2.s^{-1}$)	fu_d[e]	fu_b[f]
Desoximetasone	10.0 ± 1.5	1.8 ± 0.2	9.5 ± 2.3	2.4 ± 0.8	2.2 ± 0.6	0.054 ± 0.011	0.116 ± 0.006
Econazole	42.0 ± 3.7	1.3 ± 0.3	1.7 ± 0.6	0.44 ± 0.01	0.45 ± 0.01	0.014 ± 0.004	0.003 ± 0.0002
Hydrocortisone	48.0 ± 3.5	1.78 ± 0.08	15.9 ± 0.3	4.3 ± 0.7	4.0 ± 0.2	0.51 ± 0.055	0.72 ± 0.04
8-Methoxypsoralen	24.0 ± 1.1	1.3 ± 0.2	24.0 ± 6.0	2.2 ± 0.4	5.4 ± 0.8	0.17 ± 0.034	0.24 ± 0.03
Retinoic acid	13.0 ± 4.3	0.4 ± 0.1	0.38 ± 0.09	0.39 ± 0.05	0.5 ± 0.16	0.031 ± 0.009	0.0119 ± 0.0004
Triamcinolone acetonide	16.0 ± 4.0	1.7 ± 0.1	12.0 ± 1.0	2.8 ± 0.2	3.2 ± 0.3	0.29 ± 0.021	0.396 ± 0.007

[a] k_d distribution parameter; [b] K_m partition coefficient between donor solution and the dermis; [c] k_p dermal permeability coefficient; [d] D effective diffusion coefficient in the dermis; [e] fu_d fraction of solute unbound in the dermis; [f] fu_b = fraction of solute unbound in the blood

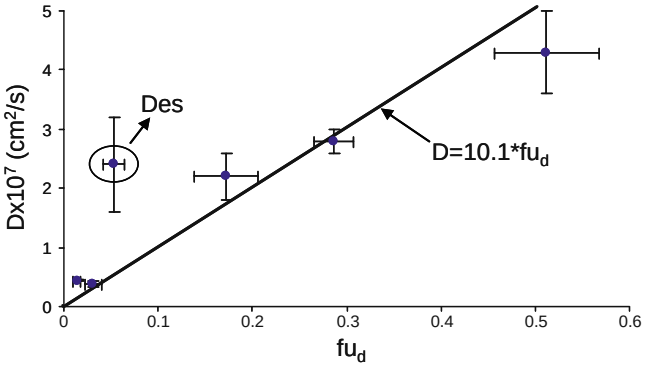

Fig. 3 Experimental diffusion coefficients *versus* fraction unbound in the dermis data. *Solid line* represents a regression with Eq. 3 where D_u is constant.

but not reduce its mobility/diffusion coefficient to the extent predicted by Eq. 3, as this equation assumes that only unbound solute is diffusing.

In Fig. 2, it was assumed that the steady state was achieved at the time of data collection. This will only be true if D_t is large enough. In previous studies (8–10), it was assumed that the transport in the dermis is solely due to solute diffusion (D_t=D). To test this assumption we substituted D_t=D in Eq. 8 and applied this transient model to the human biopsy data. The results of these regressions are shown in Fig. 4. During the regressions, parameters D, fu_b and fu_d for solutes were fixed to the values taken from Table II, and q_b and v_b were fixed to their physiological values: q_b=0.0005 s^{-1}, v_b=0.1 (19). Parameters J_0 and ps were obtained by fitting the data. It can be seen in Fig. 4 that the transient model fits were not satisfactory for four solutes (Ec, Met, RA and TA) for which application times are relatively short (about 100 min). In all these unsatisfactory regressions the transient model fails to fit concentration in the deeper layers of the dermis. This failure is most pronounced for RA. The transient model regression for Des and Hyd produced straight lines identical to the steady-state model, which is expected, as the application time was very long for these solutes (1,000 min). The unsatisfactory regression of the transient model for deeper layers is due to the assumption of the slow diffusional transport to deeper layers (D_t=D) and could not be resolved by varying parameters q_b and v_b (fits not shown). We are consequently forced to assume that the dermal transport to deeper layers is faster than molecular diffusion alone, and therefore D_t>>D. The assumption of fast dispersion transport leads to the conclusion that the solutes reach the steady state relatively early (before 100 min) and, indeed, as discussed above, provide satisfactory fits for most solutes (Fig. 2).

In Fig. 5a and b the data for parameter k_d (Table II) were analysed using Eq. 14, where it was assumed that permeability-surface area per unit volume of dermis is proportional to the octanol/water partitioning, that is ps=A×$10^{\log P}$=A×P, where A is a fitting parameter. In Fig. 5a another fitting parameter was q_b, while D_t was fixed to the molecular diffusion coefficient. It can be seen that the quality of regression is very poor, confirming the conclusion of the above analysis that transport cannot be explained by molecular diffusion alone. In Fig. 5b similar regression was performed, but D_t was given a chance to be higher, corresponding to D_t determined by blood/lymphatic transport, or equal to diffusion coefficient. In order to reduce the number of fitting parameters, it was assumed that the dispersion coefficient is the same for all solutes. The regression was significantly better compared to the case of D_t = D and resulted in all but one solute (Hyd) D_t determined by the dispersion transport with D_{disp}=5×10^{-6} cm^2s^{-1}. Other fitting parameters were A=1 and q_b=0.0014 ml s^{-1} per ml of dermis, which indicates that for all solutes $ps\,f_{ub}$>> q_b, that is, clearance is blood flow limited as described by Eq. 12. Some deviation of data in Fig. 5b is expected, given that the simplifying assumptions of equal blood flow in all the experiments (which were conducted in different subjects) were used to fit the data. The blood flow rate obtained in the regression (q_b=0.0014 ml s^{-1} per ml of dermis) is in reasonable agreement with literature data, given the variability of dermal blood flow depending on subject and experimental conditions (19).

DISCUSSION

This work shows that, for the compounds studied here in human dermis *in vivo*, the transport of the compounds into deeper tissues after topical application must involve transport into those tissues via the blood and/or lymphatics as well as by diffusion and that this transport cannot be described by dermal diffusion alone. In order for convective blood flow transport to make a significant contribution to transport to deeper tissues, there must be sufficient binding to plasma proteins and blood flow, as the surface area of blood vessels is much less than that for the dermal matrix through which diffusion transport will occur. Hence, the contribution of dermal blood flow transport is likely to be markedly reduced when there is vasoconstriction. Others have previously assumed that only molecular diffusion in the dermis has contributed to penetration to deeper layers of dermis, and therefore used the simplified model (as defined in Eq. 1) to model tissue concentration-distance profiles (8–10). In general, molecular diffusion was assumed *a priori*, in order to enable modelling in the steady state. This assumption, in turn, leads to a strong correlation between diffusion/dispersion parameter and the elimination parameter. Resolution of the actual value for either parameter is only possible if one of the parameters, dispersion or elimination, is defined and fixed. In this work,

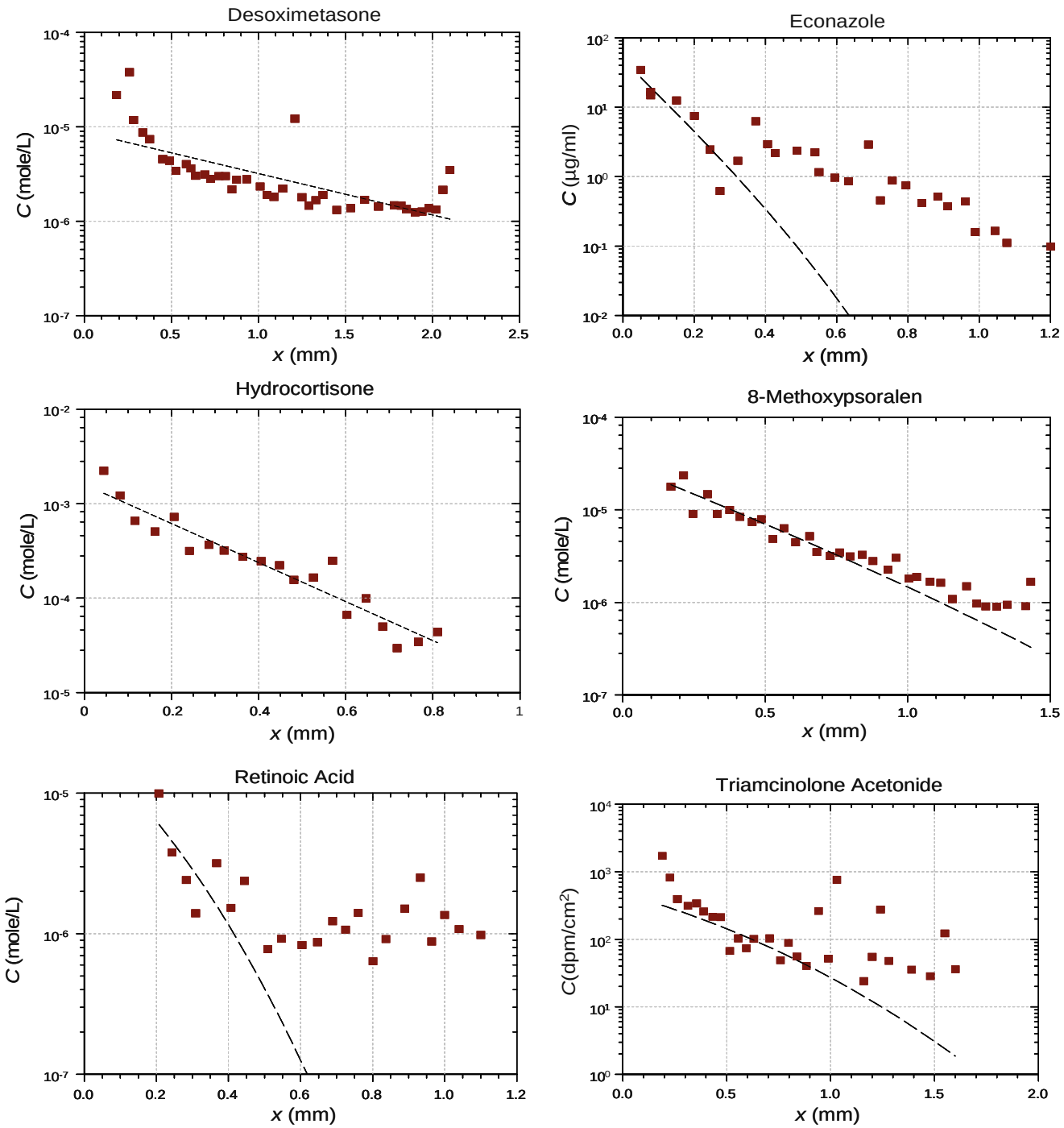

Fig. 4 The experimental data as in Fig. 2 with regression curves using the transient model (Eq. 8 with $Dt=D$, *dashed line*). For Desoximetasone and Hydrocortisone the transient and steady-state models produced identical results, as for these solutes application time is very long (1,000 min). Coefficients of determination (cd) for each of the solute's regression are as follows: Desoximetasone cd = 0.54; Econazole cd = 0.77; Hydrocortisone cd = 0.91; 8-Methoxypsoralen cd = 0.89; Retinoic acid cd = 0.30; Triamcinolone acetonide cd = 0.39.

we used the experimentally obtained *in vitro* dermal diffusion coefficient as the independently determined parameter.

The modelling dilemma addressed here is similar to one reported in the hepatic elimination literature several decades ago (20). Here, hepatic extraction data were controversially attempted to be fitted by either a well-stirred model or a tube model. An important outcome was that the intrinsic clearances obtained for highly extracted drugs estimated by the well-stirred model were several orders of magnitude different to physiologically expected values. When the actual enzymatic clearances and blood

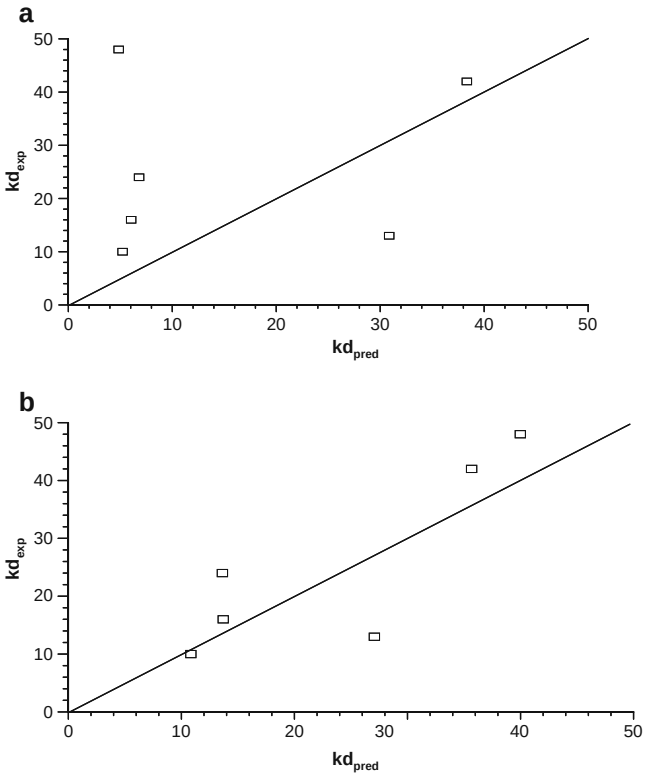

Fig. 5 Experimental *kd versus* theoretically predicted *kd* using Eq. 14 for cases of $Dt=D$ (**a**) and $Dt=Ddisp$ (**b**).

flow patterns were taken into account, a more realistic convection–dispersion model was derived (15,21). The analysis in this paper is somewhat analogous, in that our *in vitro* diffusion constants and realistic values of dermal blood flow were used to uncouple inter-dependencies between parameters. This was possible because the elimination rate (k_e in Eq. 1) in our modelling was defined for the first time in terms of physiologically based parameters such as blood flow rate (q_b), permeability surface area of blood capillaries (ps), fractions of solute unbound in the dermis (fu_d) and blood (fu_b). This allowed us to analyse dependence of elimination rate and diffusion/dispersion coefficient on the physiologically based parameters. It was concluded that the previously published *in vivo* human experimental data are not consistent with the assumption of transport in the dermis due to molecular diffusion only, and the dispersion coefficient, which is about an order of magnitude larger, has to be used instead. Our analysis suggests that transport occurs mostly by blood/lymphatic flow rather than molecular diffusion explaining the transport of solutes to deeper tissues, as assumed previously (8–10).

We note that the model, as formulated in this work, is somewhat a simplification of the physiological dermal transport and clearance. Most significantly, it was assumed that the blood flow rate per unit volume of dermis (q_b) is a constant parameter. Recent work on spatial distribution of dermal circulation (22) suggests that q_b decreases quasi-exponentially to a certain depth and is site- and skin condition-dependent. As this spatial dependence will prohibit the simple analysis of data with our model, it was considered beyond the scope of this paper. It has to be noted that this simplification will not affect the main conclusion of this paper that transport to deeper tissues is not by diffusion alone, as blood flow rate (q_b) only contributes to clearance (k_e) but not to diffusion coefficient (D). Further simplification is that, similar to the modelling of liver clearance (15), dispersion was assumed to be a constant parameter independent of other physiological parameters of the model. We have also previously related the dispersion coefficient used to describe liver elimination and transport directly to the morphology of the system and physiologically related parameters (23). The model described here for dermal transport and clearance could, in due course, be further developed more precisely to be related to the detailed morphology and physiology of the dermis and its blood vessels. However, the present model does give a global view of transport of solutes in the dermis *in vivo* being potentially either limited by dermal blood flow or by molecular diffusion in the dermis.

The proposed global model for dermal transport could be further complicated by including the concurrent transport by lymphatic flow. The extent of the contribution to the dispersion parameter from the lymphatic transport can be gained by simple analysis of data for the transport and clearance of isothiocyanate-dextran (MW = 150 kDa) in human skin (24). Figure 2 in this work shows, as a consequence of lymphatic dispersion, isothiocyanate-dextran spreads radially in the dermis a distance $\Delta d \approx$ 0.3 cm (as approximated from the figure) after $t=24$ h following intra-dermal injection. Accordingly, when a simple random walk/diffusion/dispersion process is assumed, $\Delta d \approx \sqrt{D_{lymphatic} t}$, yielding a lymphatic dispersion estimate of $D_{lymphatic} \approx 10^{-6}\mathrm{cm}^2\mathrm{s}^{-1}$. If this dermal dispersion is indicative also of the axial lymphatic transport to deeper tissues, it is more than a factor of two higher than the fastest dermal diffusion coefficient measured in this work ($D=4.3\times 10^{-7}$ $\mathrm{cm}^2\mathrm{s}^{-1}$ for hydrocortisone, see Table II). Such a difference in dispersion would be consistent with a lower variation in dermal blood flows and vessel dimensions than found for lymphatic vessels.

In this work, we have limited our analysis of dermal distribution to data obtained from human experiments after a topical application to solute concentration profiles in the dermis obtained from skin biopsy. We felt that biopsy represents a "gold standard" in measuring dermal distribution of solutes. Human dermal distribution data is also available from microdialysis experiments, and we have analysed these data separately, with similar findings. The nature of cutaneous microdialysis is such that there

are additional substantial experimental and data interpretation considerations beyond the scope and focus of this paper. Hence, we are seeking to analyse this in a separate paper. A limitation of the present analysis is the assumption of no contribution of topically absorbed drug into the systemic circulation contributing to the underlying tissue concentrations on recirculation. Our previous work has suggested that this only occurs at long times and then with most substantial contribution to tissue concentrations deep below the applied site (25), relative to the superficial tissues close to the topical application site, as studied here.

CONCLUSIONS

In this work, dermal disposition of solutes after topical application was investigated. A new two-compartment dermal clearance model that includes both transport by dermal blood vessels and by dermal diffusion was introduced to better relate dermal transport to the known dermal morphology and physiology *in vivo*. A key outcome of our analysis is that the molecular diffusion of solutes in the dermis is insufficient to alone explain solute transport to the deeper layers of dermis *in vivo*. When the contribution of dermal transport to the deeper layers due to blood or lymphatic transport is included, consistency is obtained between observed and previously described *in vivo* literature data.

ACKNOWLEDGMENTS

We are grateful to the financial support of the National Health & Medical Research Council of Australia and the Queensland and New South Wales Lions Medical Research Foundation. We also acknowledge Prof. Hans Schaefer's advice in relation to experimental data in his work.

REFERENCES

1. Schaefer H, Stuttgen G. Absolute concentrations of an antimycotic agent, econazole, in the human skin after local application. Arzneimittelforschung. 1976;26:432–5.
2. Schaefer H, Zesch A. Penetration of vitamin A acid into human skin. Acta Derm Venereol Suppl (Stockh). 1975;74:50–5.
3. Zesch A, Schaefer H. Penetration of radioactive hydrocortisone in human skin from various ointment bases. II. *In vivo*-experiments (author's transl). Arch Dermatol Forsch. 1975;252:245–56.
4. Schaefer H, Zesch A, Stuttgen G. Penetration, permeation, and absorption of triamcinolone acetonide in normal and psoriatic skin. Arch Dermatol Res. 1977;258:241–9.
5. Schaefer H, Stuttgen G, Zesch A, Schalla W, Gazith J. Quantitative determination of percutaneous absorption of radiolabeled drugs *in vitro* and *in vivo* by human skin. Curr Probl Dermatol. 1978;7:80–94.
6. Singh P, Roberts MS. Effects of vasoconstriction on dermal pharmacokinetics and local tissue distribution of compounds. J Pharm Sci. 1994;83:783–91.
7. Singh P, Roberts MS. Blood-flow measurements in skin and underlying tissues by microsphere method—application to dermal pharmacokinetics of polar nonelectrolytes. J Pharm Sci. 1993;82:873–9.
8. Gupta E, Wientjes MG, Au JL. Penetration kinetics of 2′,3′-dideoxyinosine in dermis is described by the distributed model. Pharm Res. 1995;12:108–12.
9. Cross SE, Roberts MS. Defining a model to predict the distribution of topically applied growth factors and other solutes in excisional full-thickness wounds. J Invest Dermatol. 1999;112:36–41.
10. Kretsos K, Kasting GB, Nitsche JM. Distributed diffusion-clearance model for transient drug distribution within the skin. J Pharm Sci. 2004;93:2820.
11. Kretsos K, Kasting GB. A geometrical model of dermal capillary clearance. Math Biosci. 2007;208:430–53.
12. Kretsos K, Miller MA, Zamora-Estrada G, Kasting GB. Partitioning, diffusivity and clearance of skin permeants in mammalian dermis. Int J Pharm. 2008;346:64–79.
13. Dedrick RL, Flessner MF, Collins JM, Schultz JS. Is the peritoneum a membrane? ASAIO J. 1982;1–8.
14. Danckwerts PV. Continuous flow systems: distribution of residence times. Chem Eng Sci. 1953;2:1–13.
15. Roberts MS, Rowland M. A dispersion model of hepatic elimination: 1. Formulation of the model and bolus considerations. J Pharmacokinet Biopharm. 1986;14:227–60.
16. Anissimov YG, Roberts MS. Diffusion modeling of percutaneous absorption kinetics: 4. Effects of a slow equilibration process within stratum corneum on absorption and desorption kinetics. J Pharm Sci. 2009;98:772–81.
17. Anissimov YG, Roberts MS. Diffusion modeling of percutaneous absorption kinetics: 1. Effects of flow rate, receptor sampling rate and viable epidermal resistance for a constant donor concentration. J Pharm Sci. 1999;88:1201–9.
18. Wilke CR, Chang P. Correlation of diffusion coefficients in dilute solutions. Aiche J. 1955;1:264–70.
19. Cross SE, Roberts MS. Dermal blood flow, lymphatics, and binding as determinates of topical absorption, clearance and distribution. In: Riviere JE, editor. Dermal absorption models in toxicology and pharmacology. Boca Raton: CRC Press; 2006. p. 251–82.
20. Roberts MS, Rowland M. Hepatic elimination—dispersion model. J Pharm Sci. 1985;74:585–7.
21. Cross SE, Anderson C, Roberts MS. Topical penetration of commercial salicylate esters and salts using human isolated skin and clinical microdialysis studies. Br J Clin Pharmacol. 1998;46:29–35.
22. Cevc G, Vierl U. Spatial distribution of cutaneous microvasculature and local drug clearance after drug application on the skin. J Control Release. 2007;118:18–26.
23. Anissimov YG, Bracken AJ, Roberts MS. Interconnected-tubes model of hepatic elimination. J Theor Biol. 1997;188:89–101.
24. Leu AJ, Husmann MJ, Held T, Frisullo R, Hoffmann U, Franzeck UK. Measurement of the lymphatic clearance of the human skin using a fluorescent tracer. J Vasc Res. 2001;38:423–31.